

A method for the quantitative study of atomic transitions in a magnetic field based on an atomic vapor cell with $L = \lambda$

Armen Sargsyan, Grant Hakhumyan, Aram Papoyan, David Sarkisyan*
Institute for Physical Research, Armenian Academy of Sciences, Ashtarak-0203, Armenia

Aigars Atvars, and Marcis Auzinsh
Department of Physics, University of Latvia, 19 Rainis blvd., Riga, LV-1586 Latvia
(Dated: November 12, 2018)

We describe the so-called "λ-Zeeman method" to investigate individual hyperfine transitions between Zeeman sublevels of atoms in an external magnetic field of $0.1 \text{ mT} \div 0.25 \text{ T}$. Atoms are confined in a nanocell with thickness $L = \lambda$, where λ is the resonant wavelength (794 nm or 780 nm for D₁ or D₂ line of Rb). Narrow resonances in the transmission spectrum of the nanocell are split into several components in a magnetic field; their frequency positions and probabilities depend on the B -field. Possible applications are described, such as magnetometers with nanometric spatial resolution and tunable atomic frequency references.

PACS numbers: 32.70.Jz; 42.62.Fi; 32.10.Fn; 42.50.Hz

Keywords: Atomic spectroscopy, Zeeman effect, Nanometric cell, Rb vapor, Magnetic field

It is well known that energy levels of atoms placed in an external magnetic field undergo frequency shifts and changes in their transition probabilities. These effects were studied for hyperfine (hf) atomic transitions in the transmission spectra obtained with an ordinary cm-size cell containing Rb and Cs vapor was used in [1]. However, because of Doppler-broadening (hundreds of MHz), it was possible to partially separate different hf transitions only for $B > 0.15 \text{ T}$. Note that even for these large B values the lines of ⁸⁷Rb and ⁸⁵Rb are strongly overlapped, and pure isotopes have to be used to avoid complicated spectra. In order to eliminate the Doppler broadening, the well-known saturation absorption (SA) technique was implemented to study the Rb hf transitions [2]. However, in this case the complexity of the Zeeman spectra in a magnetic field arises primarily from the presence of strong crossover (CO) resonances, which are also split into many components. That is why, as is mentioned in [2], the SA technique is applicable only for $B < 5 \text{ mT}$. The CO resonances can be eliminated with selective reflection (SR) spectroscopy [3], but to correctly determine of the hf transition position, the spectra must undergo further non-trivial processing. Another method based on the fluorescence spectrum emitted from a nanocell at thickness $L = \lambda/2$ was presented in [4]. However, in this case the sub-Doppler spectral line-width is relatively large ($\sim 100 \text{ MHz}$); also the laser power has to be relatively large to detect a weak fluorescence signal. Coherent population trapping (CPT) allows one to study the behavior of hf transitions in a magnetic field with very high accuracy (several kHz) [5], however the experimental realization is complicated; moreover, measuring hf level shifts of several GHz for $B \sim 0.1 \text{ T}$ using CPT is not realistic.

We present a method based on narrow (close to natural linewidth) velocity selective optical pumping/saturation (VSOP) resonance peaks of reduced absorption located at the atomic transitions [6]. The VSOP peaks appear

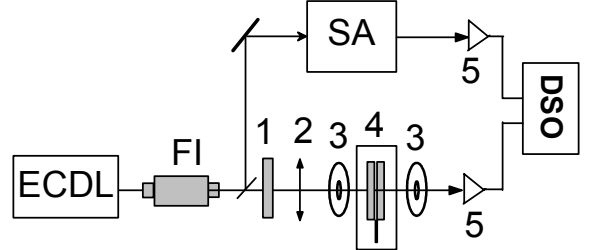


FIG. 1: Experimental setup. FI - Faraday isolator, 1 - $\lambda/4$ plate, 2 - lens ($F = 35 \text{ cm}$), 3 - ring magnets, 4 - nanocell and the oven, 5 - photodetectors, DSO-digital storage oscilloscope.

at laser intensity $\sim 1 \text{ mW/cm}^2$ in the transmission spectrum of the nanocell with atomic vapor column of thickness $L = \lambda$, where λ is the resonant wavelength of the laser radiation (794 nm or 780 nm for Rb D₁ or D₂ line). At $B > 0$, the VSOP resonance is split into several Zeeman components, the number of which depends on the quantum numbers F of the lower and upper levels. The amplitudes of these peaks and their frequency positions depend unambiguously on the B value. This so called "λ-Zeeman method" (LZM) allows one to study not only the frequency shift of any individual hf transition, but also the modification in transition probability in the region of $0.1 \text{ mT} \div 0.25 \text{ T}$ (LZM is expected to be valid up to several T).

Experimental realization of LZM is simple enough (see Fig.1). The circularly polarized beam of an extended cavity diode laser (ECDL, $\lambda = 794 \text{ nm}$, $P_L \sim 5 \text{ mW}$, $\gamma_L < 1 \text{ MHz}$) resonant with the ⁸⁷Rb D₁ transition frequency, after passing through Faraday isolator, was focused ($\oslash 0.5 \text{ mm}$) onto Rb nanocell with a vapor column of thickness $L = \lambda$ at an angle close to normal. The design of

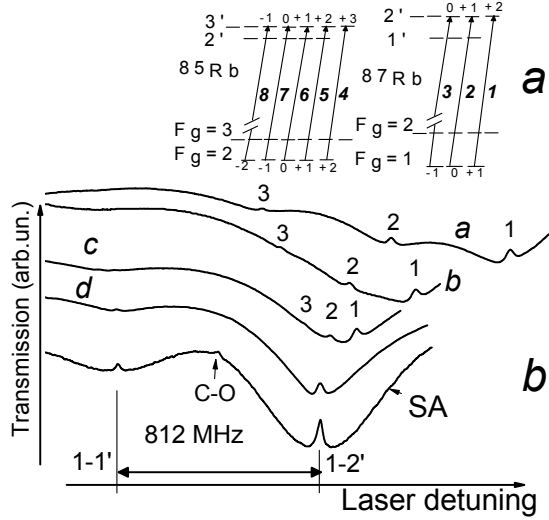


FIG. 2: a) ^{87}Rb , ^{85}Rb D₁ line atomic transitions, σ^+ excitation; b) $F_g = 1 \rightarrow F_e = 1,2$ transmission spectra for $B = 59$ mT (a), 31 mT (b), 11.5 mT (c), and 0 (d); lower curve is SA spectrum.

a nanocell is presented in [6]. The source temperature of the atoms of the nanocell was 110 °C, corresponding to a vapor density $N \sim 10^{13} \text{ cm}^3$, but the windows were maintained at a temperature that was 20 °C higher. Part of the laser radiation was diverted to a cm-size Rb cell to obtain a $B = 0$ SA spectrum, which served as frequency reference. The nanocell transmission and SA spectra were detected by photodetectors and recorded by a digital storage oscilloscope. Small longitudinal magnetic fields ($B < 25$ mT) were applied to the nanocell by a system of Helmholtz coils (not shown in Fig.1). The B -field strength was measured by a calibrated Hall gauge. Among the advantages of LZM is the possibility to apply much stronger magnetic fields using widely available strong permanent ring magnets (PRM). In spite of the strong inhomogeneity of the B -field (in our case it can reach 15 mT/mm), the variation of B inside the atomic vapor column is a few μT , i.e., by several orders less than the applied B value because of the small thickness of the nanocell (794 nm). The allowed transitions between magnetic sublevels of hf states for the ^{87}Rb D₁ line in the case of σ^+ (left circular) polarized excitation are depicted in Fig. 2a (LZM also works well for σ^- excitation). Fig. 2b shows the nanocell transmission spectra for the $F_g = 1 \rightarrow F_e = 1,2$ transitions at different values of B (the labels denote corresponding transitions shown in Fig.2a). As it is seen, all the individual Zeeman transitions are clearly detected. The two transitions $F_g = 1 \rightarrow F_e = 1$ (not shown in Fig. 1a) are detectable for $B < 12$ mT, while at higher B their probabilities are strongly reduced (this is also confirmed theoretically [4]). Note that the absence of CO resonances in transmission spectra is

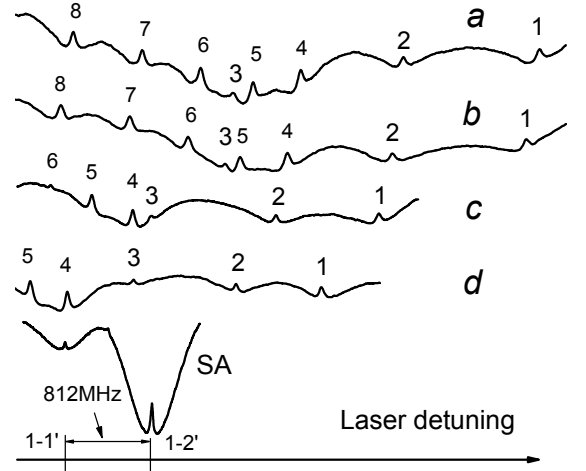


FIG. 3: Transmission spectra for $B = 0.24$ T (a), 0.23 T (b), 0.154 T (c), 0.117 T (d) ; lower curve is SA spectrum.

an important advantage of the nanocell [6].

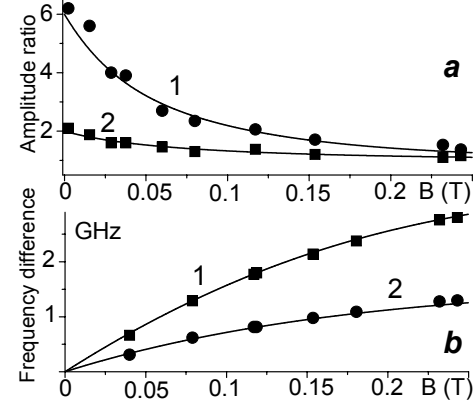


FIG. 4: a) (1) - ratio $A(1)/A(3)$, (2) - ratio $A(1)/A(2)$ versus B ; b) (1) - $\Delta(1,3)$, (2) - $\Delta(1,2)$ versus B .

Transmission spectra for larger B values are presented in Fig. 3 (also for Zeeman transitions of the ^{85}Rb D₁ line). The strong magnetic field was produced by two $\odot 30$ mm PRMs with $\odot 3$ mm holes to allow radiation to pass placed on opposite sides of the nanocell oven and separated by a distance that was varied between 35 and 50 mm (see Fig. 1). To control the magnetic field value, one of the magnets was mounted on a micrometric translation stage for longitudinal displacement. In particular, the B -field difference of curves (a) and (b) is obtained by a PRM displacement of 0.67 mm, corresponding to a

rate of 15 mT/mm. The frequency difference between the VSOP peaks numbered 4 (curves (a), (b)) for this case is 100 MHz. By a 20 μ m displacement of the PRM it is easy to detect \sim 3 MHz frequency shift of peak 4. The advantage of submicron-size magnetic field probe can be fully exploited for the case of larger B -field gradient, as well as after further optimization of the method (reduction of laser intensity, implementation of frequency modulation and lock-in detection, etc.). An important advantage of LZM is that the amplitude of VSOP peaks is linearly proportional to the corresponding Zeeman transition probability, which offers the possibility to quantitatively study the modification of individual Zeeman transition probabilities in a magnetic field. Thus, in weak magnetic fields ($B \sim 0$), the probabilities of transitions labeled 1, 2, and 3 compose the ratio 6:3:1, which varies rapidly as B increases. Fig. 4a presents the amplitude ratio $A(1)/A(3)$ (curve 1) and $A(1)/A(2)$ (curve 2) as a function of B (hereafter the dots and solid lines denote experiment and theory, respectively). Fig. 4b shows the frequency difference $\Delta(1,3)$ and $\Delta(1,2)$ between transitions labeled 1 and 3 (curve 1) and 1 and 2 (curve 2) as a function of B . Obviously, by measuring $\Delta(1,3)$ and $\Delta(1,2)$ it is possible to determine the strength of magnetic field, even in the absence of reference spectra.

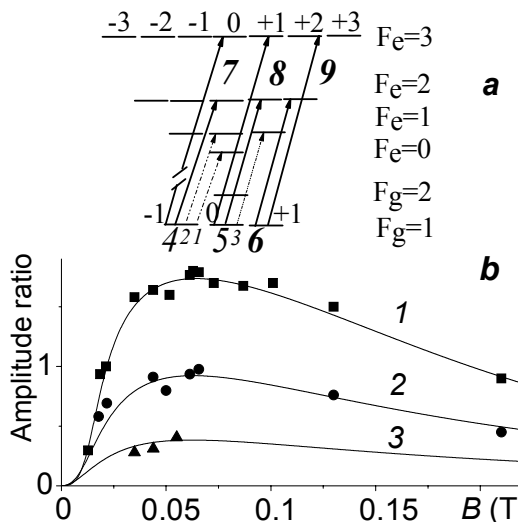


FIG. 5: a) ^{87}Rb D₂ line atomic transitions, σ^+ excitation; b) (1) - ratio A(7)/A(6), (2) - ratio A(8)/A(6), (3) - ratio A(9)/A(6) versus B.

We also implemented LZM to study transitions $Fg=1 \rightarrow Fe=0,1,2,3$ of the ^{87}Rb D₂ line ($\lambda = 780$ nm; all the other experimental parameters and conditions are the same). The possible Zeeman transitions for σ^+ polarized excitation are depicted in Fig. 5a. Particularly, it

was revealed that for $B > 10$ mT, also the ${}^{87}\text{Rb}$ D_2 , $F_g=1 \rightarrow F_e=3$ "forbidden" transitions (labeled 7,8,9) appear in spectrum, for which new selection rules with respect to the quantum number F apply. Moreover, for 20 mT $< B < 0.2$ T the probability of transition 7 exceeds that of 6, the strongest transition at $B = 0$. Fig. 5b gives the B -field dependence of amplitude (transition probability) ratio $A(7)/A(6)$, $A(8)/A(6)$, and $A(9)/A(6)$ (curves 1,2,3). Both in Fig. 4a and Fig. 5b, there is good agreement between experiment and theory. The nanocell transmission spectrum for these transitions at $B = 0.21$ T is presented in Fig. 6. The two arrows show the positions of the ${}^{85}\text{Rb}$ $F_g=2 \rightarrow F_e=4$ Zeeman transitions (theory [4] well predicts that their probabilities have to be small). The upper insets show the B -field

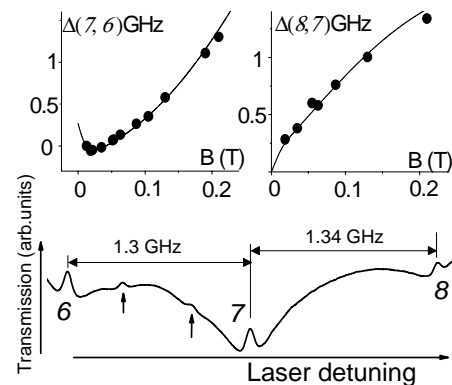


FIG. 6: Transmission spectrum, $B = 0.21$ T; upper insets: $\Delta(7,6)$ (left), and $\Delta(8,7)$ (right) versus B .

dependence of $\Delta(7,6)$ and $\Delta(8,7)$. We should note that transition 7 is strongly shifted (by 5.6 GHz) from the $B = 0$ position of the $F_g=1 \rightarrow F_e=2$ transition. The latter allows development of a frequency reference based on a nanocell and PRMs, widely tunable over a range of several GHz by simple displacement of the magnet. LZT can be successfully implemented also for studies of the D₁ and D₂ lines of Na, K, Cs, and other atoms.

Acknowledgements

This work is partially supported by INTAS South-Caucasus Grant 06-1000017-9001 and by SCOPES Grant IB7320-110684/1. We acknowledge support from the ERAF grant VPD1/ERAF/CFLA/05/APK/2.5.1./000035/018, and A.A acknowledges support from the ESF project.

E-mail of David Sarkisyan: david@ipr.sci.am.

[1] P. Tremblay, A. Nichaud, M. Levesque, S. Treriault, M. Breton, J. Beaubien, N. Cyr, *Phys. Rev. A* **42** (1990).

[2] M.U. Momeen, G. Rangarajan, P.C. Deshmukh, *J. Phys. B: At. Mol. Opt. Phys.* **40**, 3163 (2007).

[3] N. Papageorgiou, A. Wies, V. Sautenkov, D. Bloch, M. Ducloy, *Appl. Phys. B* **59**, 123 (1994).

[4] D. Sarkisyan, A. Papoyan, T. Varzhapetyan, J. Alnis, K. Blush, M. Auzinsh, *J. of Opt. A: Pure and Appl. Opt.* **6**, S142 (2004); D. Sarkisyan, A. Papoyan, T. Varzhapetyan, K. Blush, M. Auzinsh, *JOSA B* **22**, 88 (2005).
The relative transition probability and magnetic sublevel energy simulation in the magnetic field is based on the eigenvalue and eigenvector dependence from the magnetic field calculation of the Hamilton matrix for the full hfs manifold.

[5] R. Wynands, A. Nagel, *Appl. Phys. B: Las. Opt.* **68**, 1 (1999).

[6] D. Sarkisyan, T. Varzhapetyan, A. Sarkisyan, Yu. Malakyan, A. Papoyan, A. Lezama, D. Bloch, M. Ducloy, *Phys. Rev. A* **69**, 065802 (2004); C. Andreeva, S. Cartaleva, L. Petrov, S.M. Saltiel, D. Sarkisyan, T. Varzhapetyan, D. Bloch, M. Ducloy, *ibid.* **76**, 013837 (2007) and references therein; A. Sargsyan, D. Sarkisyan, A. Papoyan, Y. Pashayan-Leroy, P. Moroshkin, A. Weis, A. Khanbekyan, E. Mariotti, L. Moi, to be published in *Laser Phys.* (2008).